

A new approach in rock-typing, documented by a case study of layer-cake reservoirs in field "A", offshore Abu Dhabi (U.A.E.)

Bruno GRANIER¹

Abstract: In carbonate reservoirs, the relationship between porosity \emptyset , a measure of the combined volumes of several kinds of pore space (e.g. interparticle and separate-vug), and permeability K are neither linear nor logarithmic, hence only weakly correlatable. Approaches to an estimation of permeability that employ both petrographical and petrophysical parameters, the so-called rock-typing techniques, have proven to be the most nearly precise. However in many studies simple K/ \emptyset cross-plots are used for each rock-type to provide trendlines from which K values are derived as a function of \emptyset values; this is common practice even though the coefficient of correlation r^2 departs significantly from 1.

This paper describes and provides examples of an improved technique of rock-type classification in which each rock-type is characterized by a discrete and unique Gaussian distribution of log K. It facilitates upscaling for it suggests the use of a single geometric mean value for permeability and a corresponding standard deviation (variance, or coefficient of variation) for each rock-type.

This new technique can be used in uncored wells by extrapolating these determinations into wireline logs as documented below in a case study of layer-cake reservoirs in a field of the Abu Dhabi offshore (U.A.E.).

Key Words: Petrophysics; sedimentary petrography; limestone; dolomite; chalk; rock-typing; porosity; permeability; rock-type; Abu Dhabi

Citation: GRANIER B. (2003).- A new approach in rock-typing, documented by a case study of layer-cake reservoirs in field "A", offshore Abu Dhabi (U.A.E.).- [Carnets de Géologie / Notebooks on Geology](#), Maintenon, Article 2003/04 (CG2003_A04_BG)

Résumé : Une nouvelle approche du 'rock-typing', illustrée par l'étude de réservoirs de type 'mille-feuille' du champ "A", domaine maritime d'Abou Dabi (Émirats Arabes Unis).- Dans les réservoirs carbonatés, la porosité \emptyset , résultant du cumul de différents types de volume de pores (volume interparticulaire ou vacuoles non connectées, par exemple), et la perméabilité K sont deux paramètres pétrophysiques faiblement corrélés. Aussi, parmi les différentes approches utilisées pour estimer la perméabilité, celles qui combinent les paramètres pétrographiques avec les paramètres pétrophysiques, connus sous le vocable de techniques de 'rock-typing', ont fourni les résultats les plus probants. Toutefois dans de nombreux cas, de simples graphiques K/ \emptyset sont encore utilisés pour obtenir pour chaque 'rock-type' une fonction exponentielle ou logarithmique à partir de laquelle les valeurs de K seront calculées en fonction de celles de \emptyset : ceci reste encore une règle quasi générale, même lorsque le coefficient r^2 s'écarte significativement de 1.

Le présent travail propose une approche basée sur une technique plus sophistiquée de classification en groupes pétro-physico-graphiques, dans laquelle chaque famille est caractérisée par une distribution 'log normale' de K. Cette technique facilite les changements d'échelle puisque elle suggère d'utiliser pour chaque 'rock-type' la moyenne géométrique et le coefficient de corrélation correspondant (variance ou écart-type) pour les valeurs de perméabilité.

Elle peut être appliquée avantageusement dans des puits non carottés en extrapolant la géologie grâce aux logs électriques. A titre d'exemple, cette technique a été appliquée aux réservoirs de type 'mille-feuille' du champ "A" (Abou Dabi, Émirats Arabes Unis).

Mots-Clefs : Pétrophysique ; pétrographie sédimentaire ; calcaire ; dolomie ; craie ; rock-typing ; porosité ; perméabilité ; rock-type ; Abou Dabi

Introduction

In his pioneering work, G.E. ARCHIE (1950) sets out the fundamentals of rock-type classification. Any porous network is related to its host rock fabric; therefore petrophysical parameters, such as porosity (\emptyset), permeability (K), and saturation (S), for any given "type of rock" are controlled by pore sizes and their

distribution and interconnection. The goal of reservoir characterization is to predict the spatial distribution of such petrophysical parameters on a field scale.

In field "A", offshore Abu Dhabi (United Arab Emirates), the interval studied consists of a series of layer-cake reservoirs bracketed by a shale-dominated formation "A" above, which forms the regional seal, and a mainly dense

¹ ADMA-OPCO, P.O. Box 303, Abu Dhabi (United Arab Emirates);
present address: Total, DGE/GSR/VdG, Tour Coupole, 2 Place de Coupole, La Défense 6 - Cédex 4,
92078 Paris La Défense (France)
[Bruno.Granier@Total.com](mailto: Bruno.Granier@Total.com)
Manuscript online since July 12, 2003

limestone-dominated formation "F" below (LYON *et alii*, 1998). In terms of reservoir, it has been divided into 4 main zones (Fig. 1) denominated from the top down "B" to "E". Sequence stratigraphy helped delineate 16 "operational" units (Fig. 1), of which the limits are sequence boundaries, transgressive surfaces, or maximum flooding surfaces. The layering used in the latest reservoir model is based on a combination of the overall stratigraphic framework and the characteristics of the reservoir rocks. It consists of ten layers from top to bottom (Fig. 1):

- Layer 1, "B",
- Layer 2, "C",
- Layer 3, "C-tight" *pars*,
- Layer 4, "C-tight" *pars*,
- Layer 5, "D" *pars*,
- Layer 6, "D" *pars*,
- Layer 7, "D" *pars*,
- Layer 8, "D" *pars* and "E-tight",
- Layer 9, "E" *pars*,
- Layer 10, "E" *pars*.

Zones	Operational Units	Rock-/Litho- Types	Layers
A	0	RO (shale)	0
B	1	R-chalk	1
	2		
	3		
	4		
	5		
C	6	RR-0.25	2
	7	RO (shale)	3
	8	RO (grain)	4
D	9	RR-0.45	5
	10	R-stylo	6
	11	RR-0.45	7
	12	RO (crypto)	8
E	13	RR-0.45	9
	14		10
	15		11
F	16	RO (grain)	11
	17	RO (crypto + S.V.)	

Figure 1: Relationships of operational units and rock-/litho- types to reservoir layers.

Although sequence stratigraphy helps to establish a geologically valid reservoir framework, rock-types are the building blocks that complete the construction of reservoir models. This study focuses on these building blocks and more precisely on their petrophysical parameters.

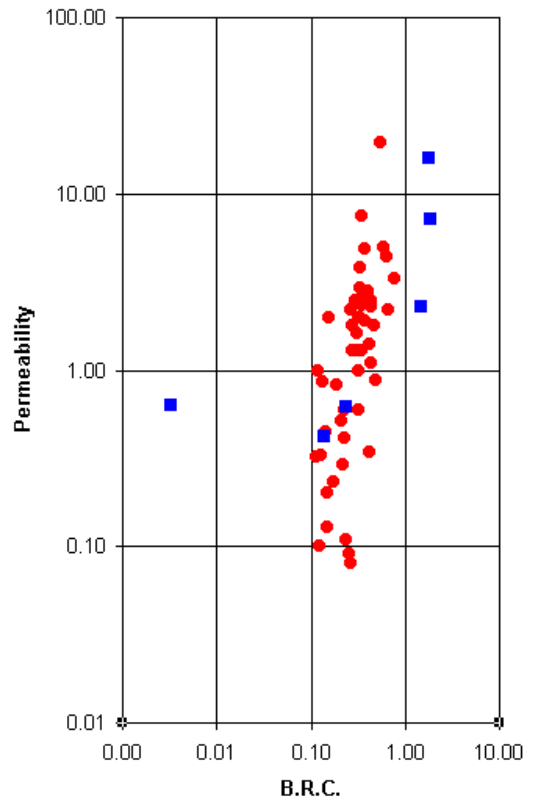


Figure 2: BRC/K cross-plot for the 65 samples used for Hg injection. Caption: blue squares = discarded samples; red dots = remaining samples.

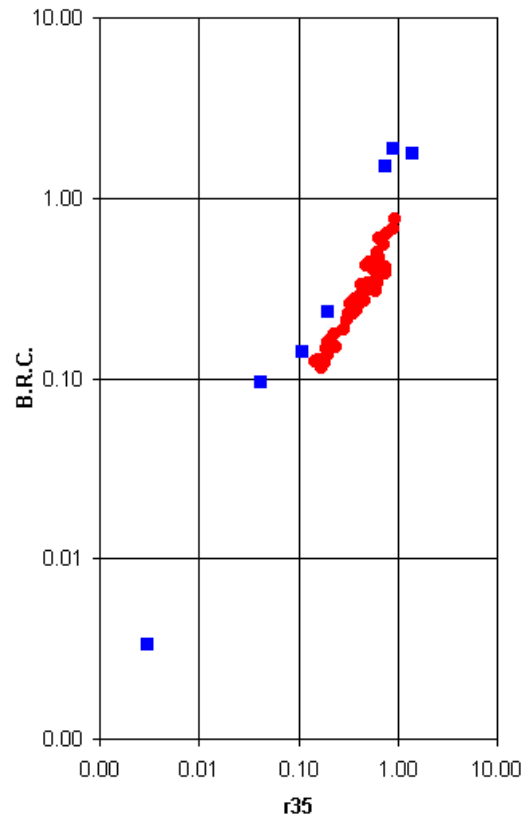


Figure 3: BRC/K cross-plot for the 65 samples used for Hg injection. Caption: blue squares = discarded samples; red dots = remaining samples. The program found a linear correlation between the two parameters with $r_{35} = 1.25 \text{ BRC} + 0.07$ with $r^2 = 0.86$.

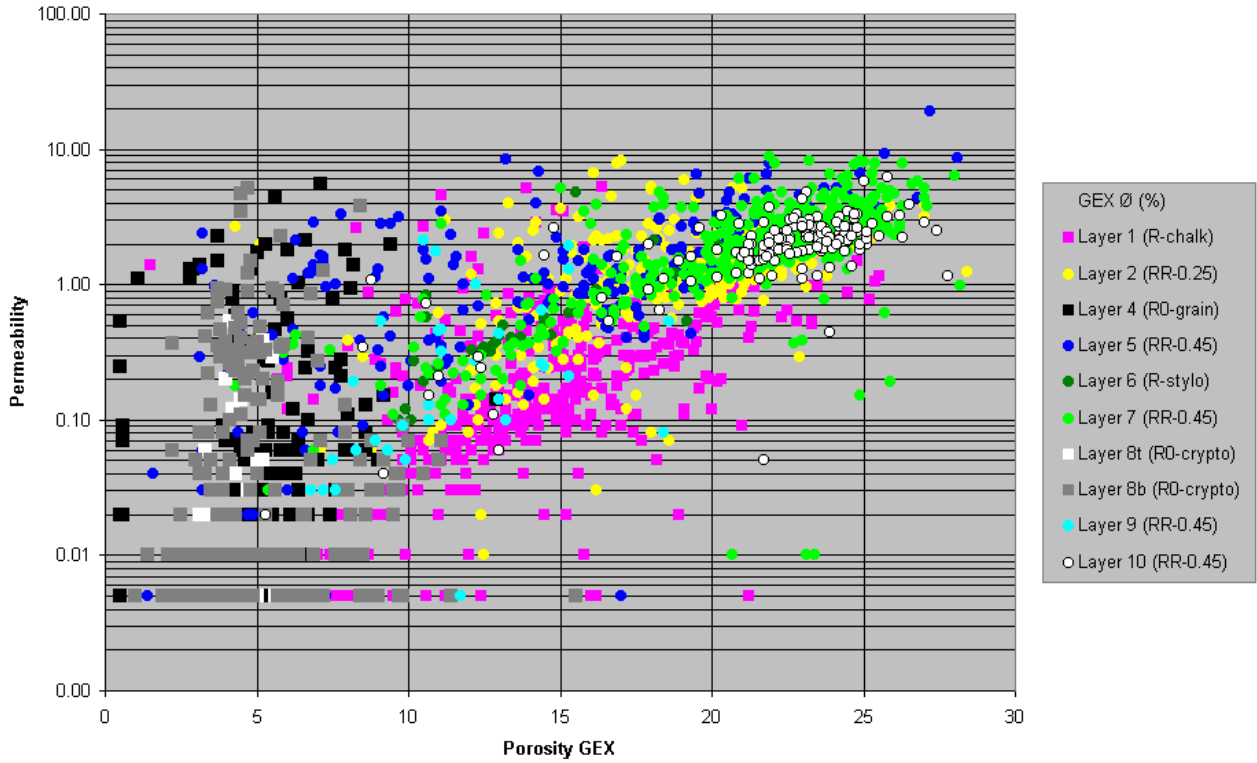


Figure 4: K/Ø cross-plot per layer (*i.e.* by "dominant" rock-type). All samples with a GEX (Gas Expansion) porosity.

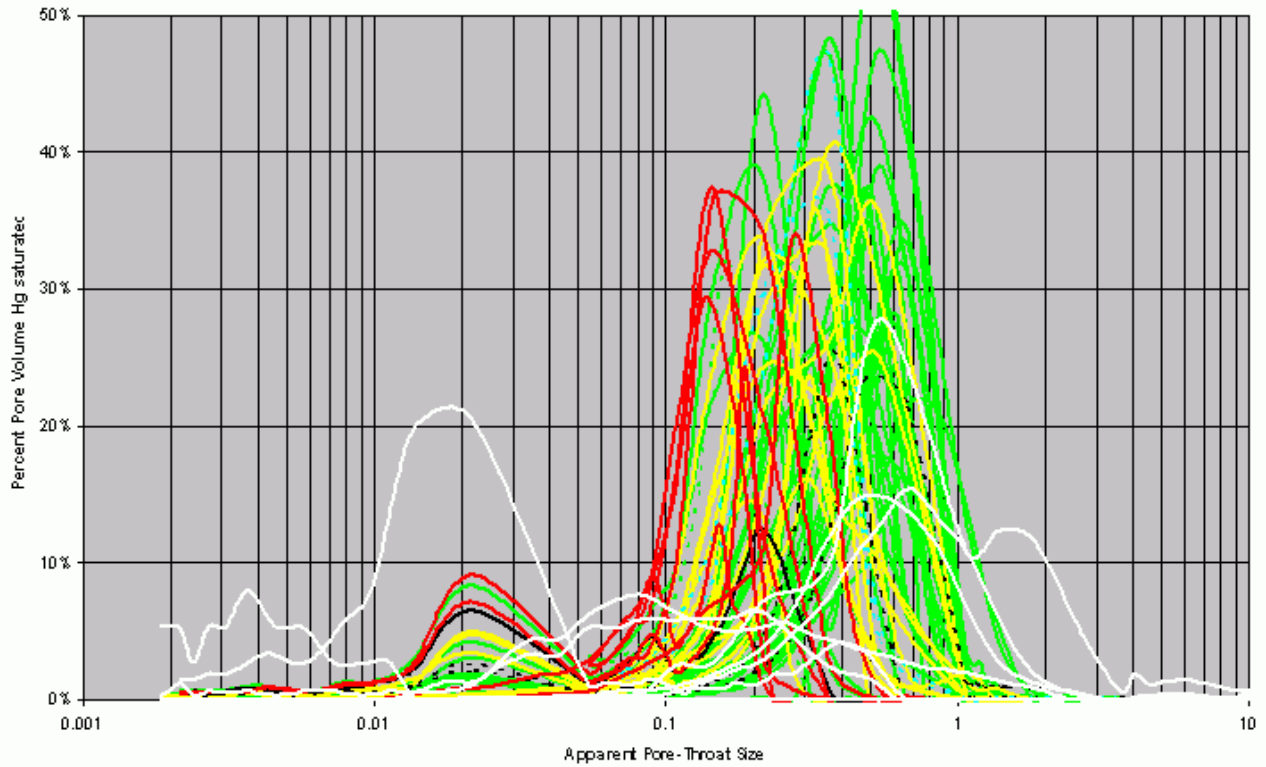


Figure 5: Hg injection data: "apparent pore-throat-size" (μm) versus "pore volume Hg saturatec" (%). Key: red for R-chalk ("B"); yellow for RR-0.25 ("C"); green for RR-0.45 ("D-E"); white for discarded samples. These should be plotted as histograms; curves are used only for display!

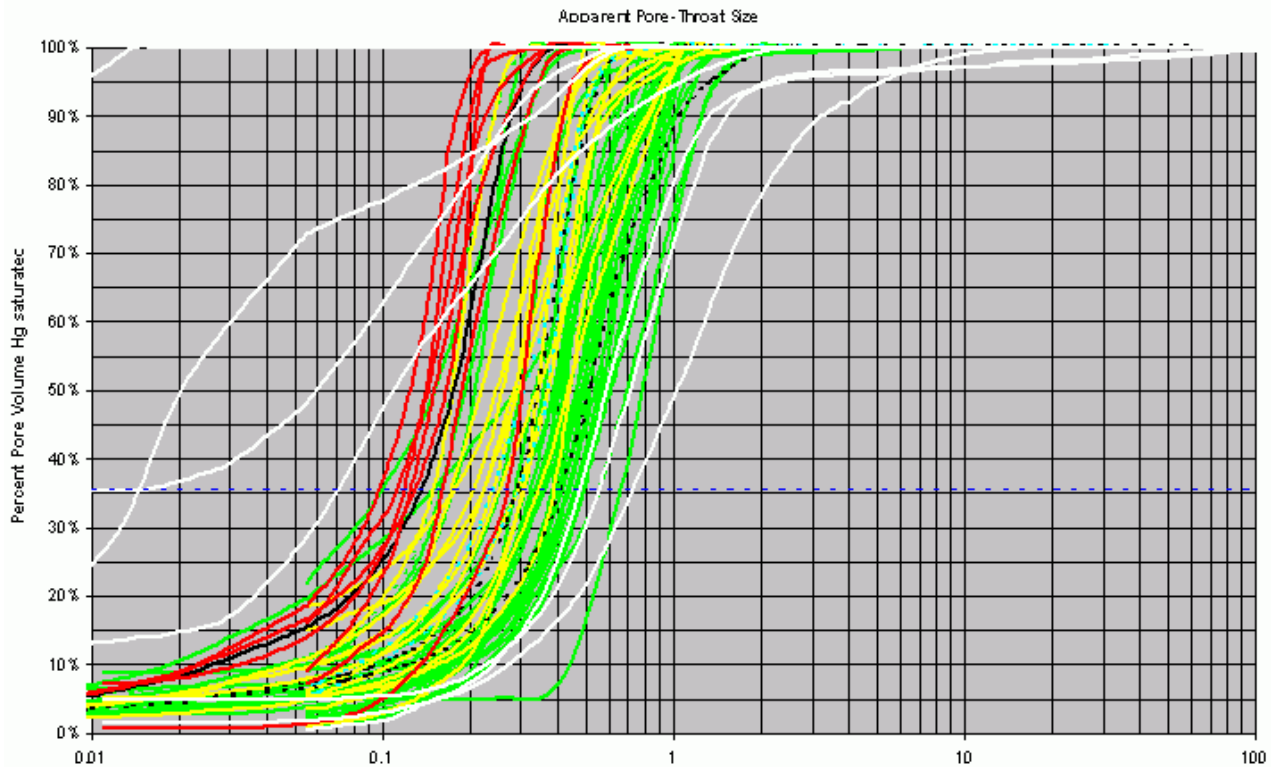


Figure 6: Hg injection data: "apparent pore-throat-size" (μm) versus "pore volume Hg saturated" (%), cumulative. Dashed horizontal line at 35% Hg injection. These should be histograms; curves are used only for display!

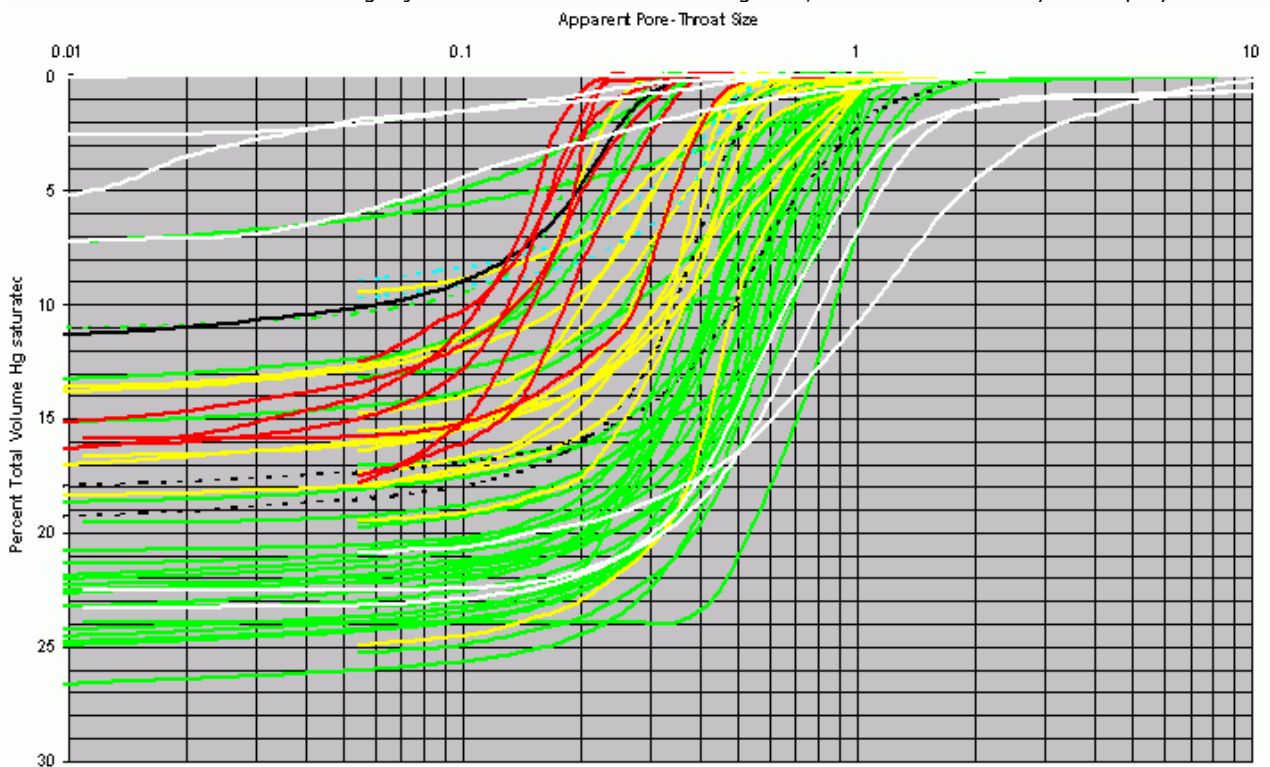


Figure 7: Hg injection data: "apparent pore-throat-size" (μm) versus "total volume Hg saturated" (%), cumulative. These should be histograms; curves are used only for display!

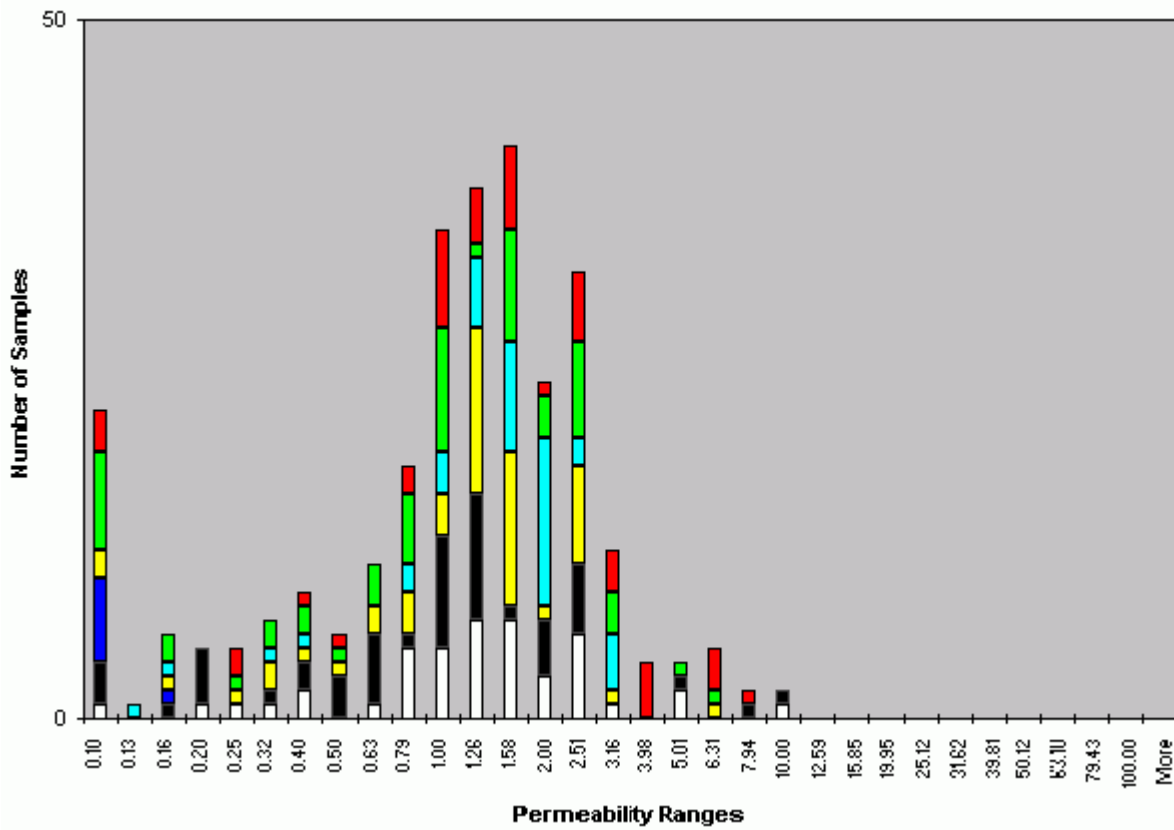


Figure 8: Permeability histogram for RR-0.25 ("C") in layer 2 (all wells).

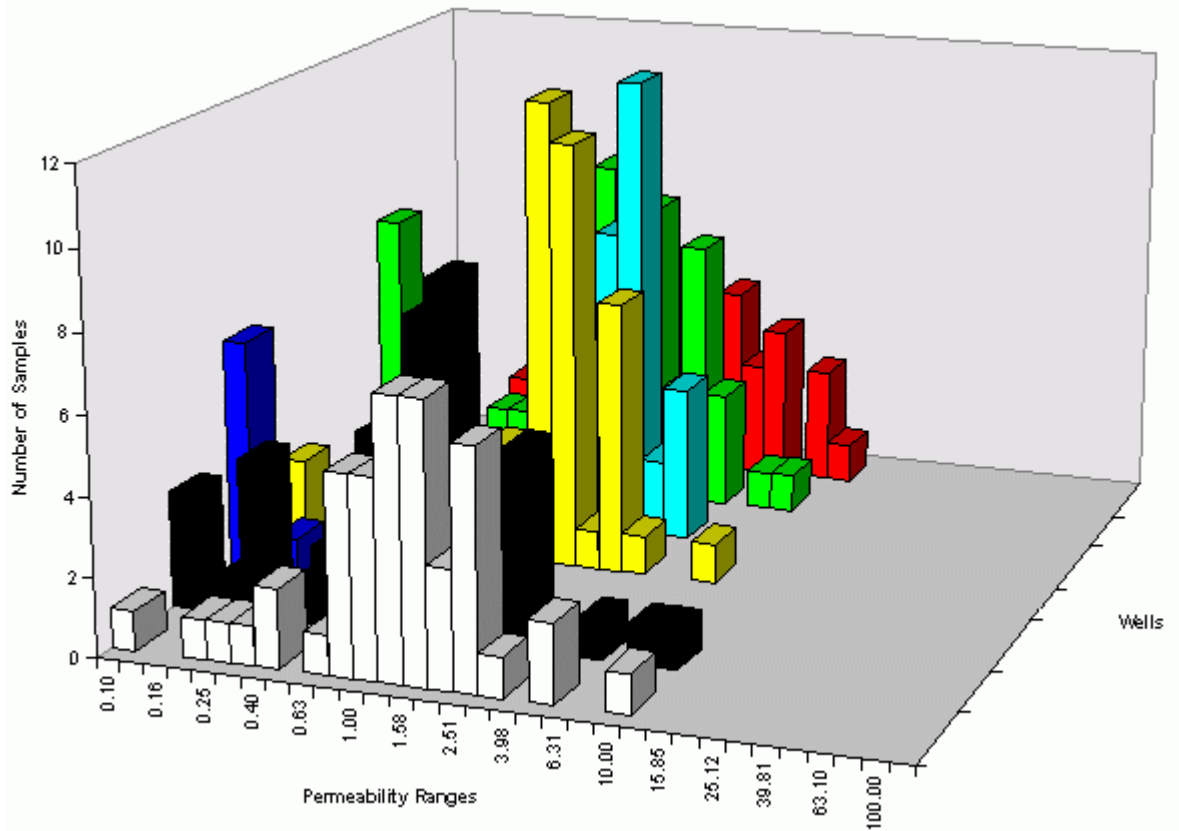


Figure 9: Permeability histograms for RR-0.25 ("C") in layer 2 (each well).

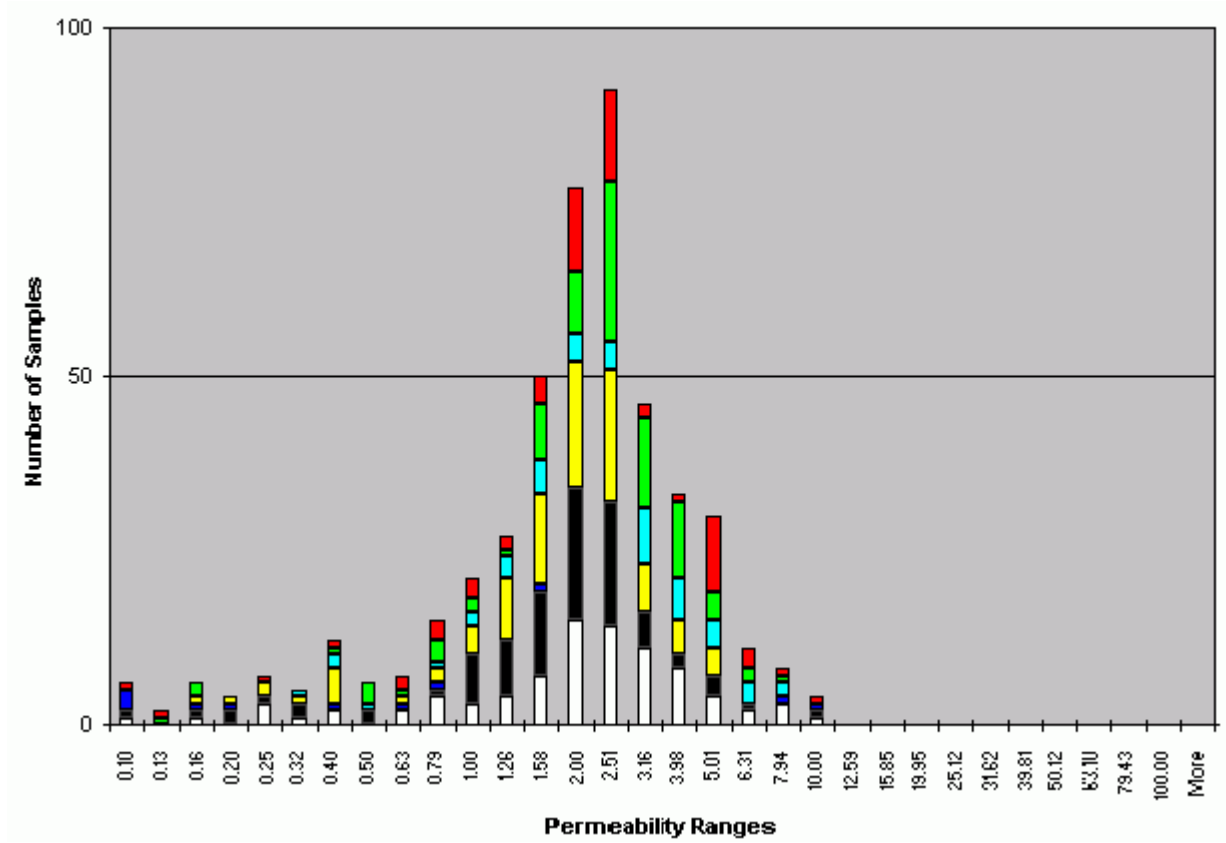


Figure 10: Permeability histogram for RR-0.45 ("D") in layer 7 (all wells).

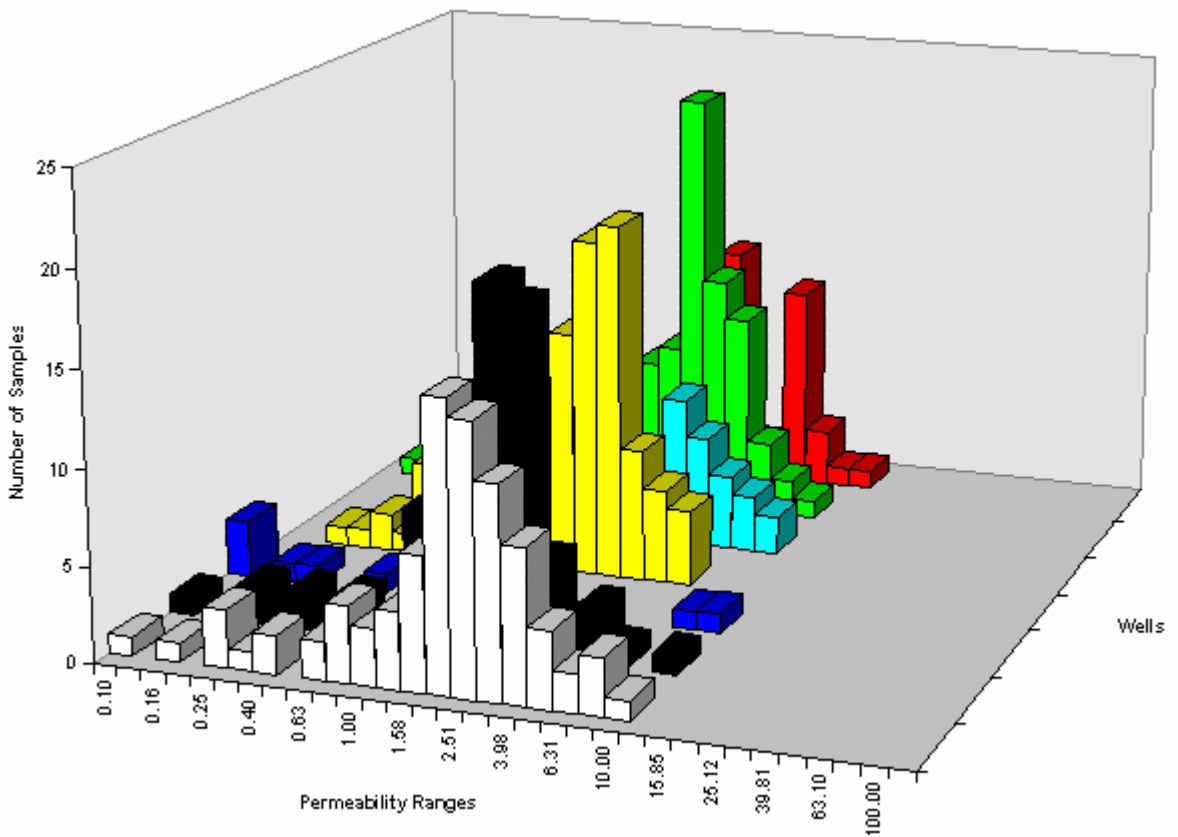


Figure 11: Permeability histograms for RR-0.45 ("D") in layer 7 (each well).

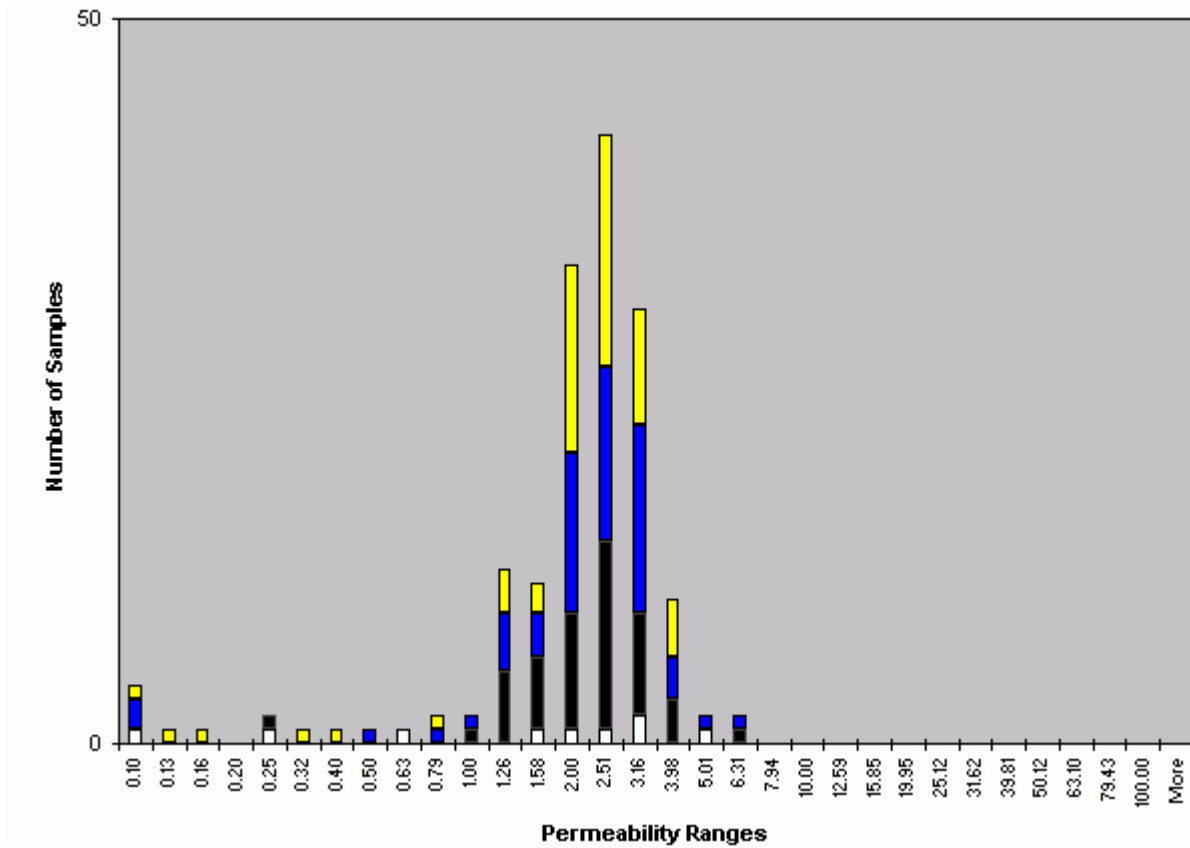


Figure 12: Permeability histogram for RR-0.45 ("E") in layer 10 (all wells).

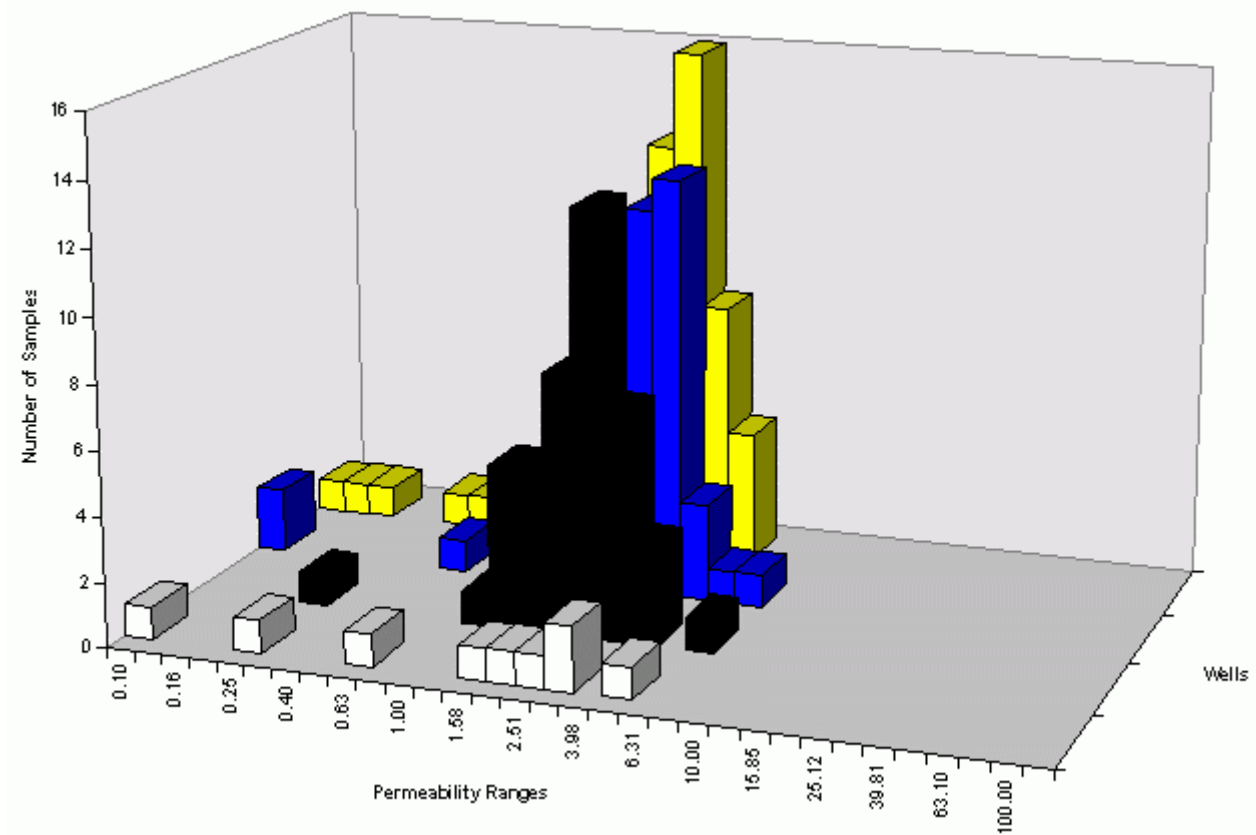


Figure 13: Permeability histograms for RR-0.45 ("E") in layer 10 (each well).

In his examination of the "rock type-porosity-permeability relation", G.E. ARCHIE (1950) stated that "a broad relationship exists between porosity and permeability of a formation" (a "formation" *sensu* G.E. ARCHIE is a "type of rock" or "rock-type"). In his conclusions he wrote, "The relations between rock characteristics should be thought of as trends" and added, "Actually, these may be expressed by mathematical formulae". Neglecting the other conclusions of this seminal paper later workers drew trendlines on K/\emptyset cross-plots and then used K/\emptyset transforms to predict K from either the total or the effective \emptyset . The present study addresses a different approach to the "rock type-porosity-permeability relation".

Summary of the methodology

By definition, setting up a classification of rock-type in subsurface reservoirs must be based on cores. The approach is basically in 3 steps. First the several fabrics are identified using thin section and conventional core analyses. Then (or at the same time) the preliminary types thus classified must be related to Hg injection curves. In field "A", our database includes:

- the rock-fabric (some 5000 thin sections have been analyzed),
- the porosity range (some 2700 GEX / Helium \emptyset and 2700 FLD \emptyset measurements were available),
- the permeability range (some 3350 K measurements were available), and
- the pore-throat size distribution derived from the Hg injection curves (65 P_c curves were available: Table 1, Fig. 3-7).

When such a procedure has been carried out for cored intervals, it should be possible to extrapolate it to other wells and to uncored intervals using wireline information. In this study, statistical analyses of available data were undertaken before this last step took place because they have helped greatly in making a definitive rock-type classification.

Preliminary rock-typing (from thin sections and conventional core analyses)

First, it should be pointed out that in our reservoirs there is little separate-vug porosity. In any case, separate vugs do not contribute significantly to permeability (LUCIA, 1983).

Second, some permeability measurements must be discarded. Contractor plug descriptions often mention the occurrence of joints (stylolite, fracture, *etc.*). In such cases measured permeabilities may be greater by a factor of ten to a hundred than those obtained from samples

with similar fabrics but lacking these phenomena. In this study, most K values higher than 5 mD are the result of plug failure during or before the measurement. Commonly they represent less than 3 per cent of the samples.

Third, a plug is not necessarily homogenous; it may include several rock-fabrics (*e.g.* burrows, boundstone with matrix, ...). Therefore measurements made on a heterogeneous plug should not be taken into account, even if the thin section displays only one texture. For example, plugs taken from the Rudist facies of zones "C" to "E" commonly include large shell fragments, so the matrix permeability (*i.e.* host rock permeability) may be grossly undervalued by conventional measurements ("Comet effect" on K/\emptyset frequency maps per layer or on K/\emptyset cross-plot: Fig. 4; "Manhattan effect" on 3D K/\emptyset histograms: Fig. 14-15).

As a matter of fact, the range of permeabilities encountered in this reservoir study is very limited; consequently this small breadth of field restricts the range in which the several rock-types can be defined. Conventional core studies and petrographical analyses available for some 5000 samples have led to the differentiation of 3 groups of lithotypes / rock-types:

1. of very low permeability values ($K < 0.5$ mD²) and low porosity values ($\emptyset < 10\%$),
2. of very low permeability values ($K < 0.5$ mD) and fair to high porosity values ($\emptyset > 10\%$),
3. of low permeability values (0.5 mD $< K < 5$ mD).

Each of these three groups is comprised of 1 to 4 lithotypes.

The first group is made up of 4 lithotypes, the poorest in terms of reservoir characteristics:

- **RO-shale**, the shale. It is characteristic of the shale-dominated formation "A" above the studied interval. It is also found mainly in layer 3; there it forms the upper part of the dense interval, formerly designated "C-tight", which constitutes the effective barrier between the so-called "B" and "C" reservoirs;
- **RO-grain**, the cemented grain-dominated textures. It occurs mainly in layer 4; there it forms the lower part of the dense interval, the former "C-tight", between the so-called "B" and "C" reservoirs. The grain-dominated textures

² Darcy = 0.9869 μm^2 .

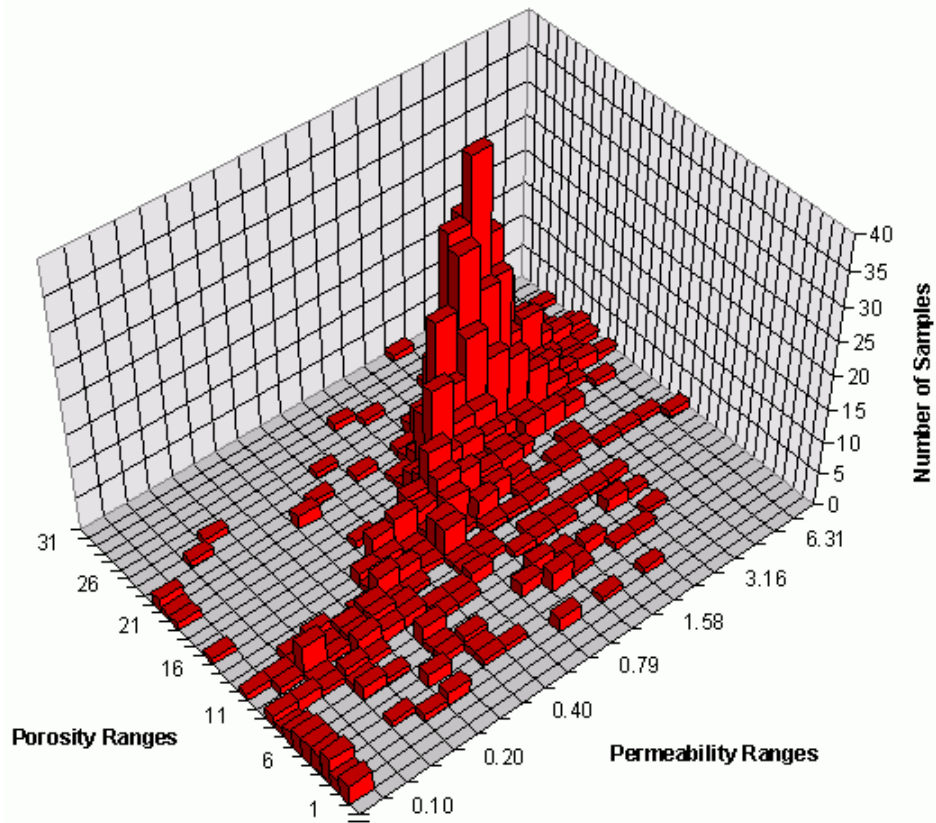


Figure 14: 3D K/Ø histogram for RR-0.45 ("D-E") (901 samples).

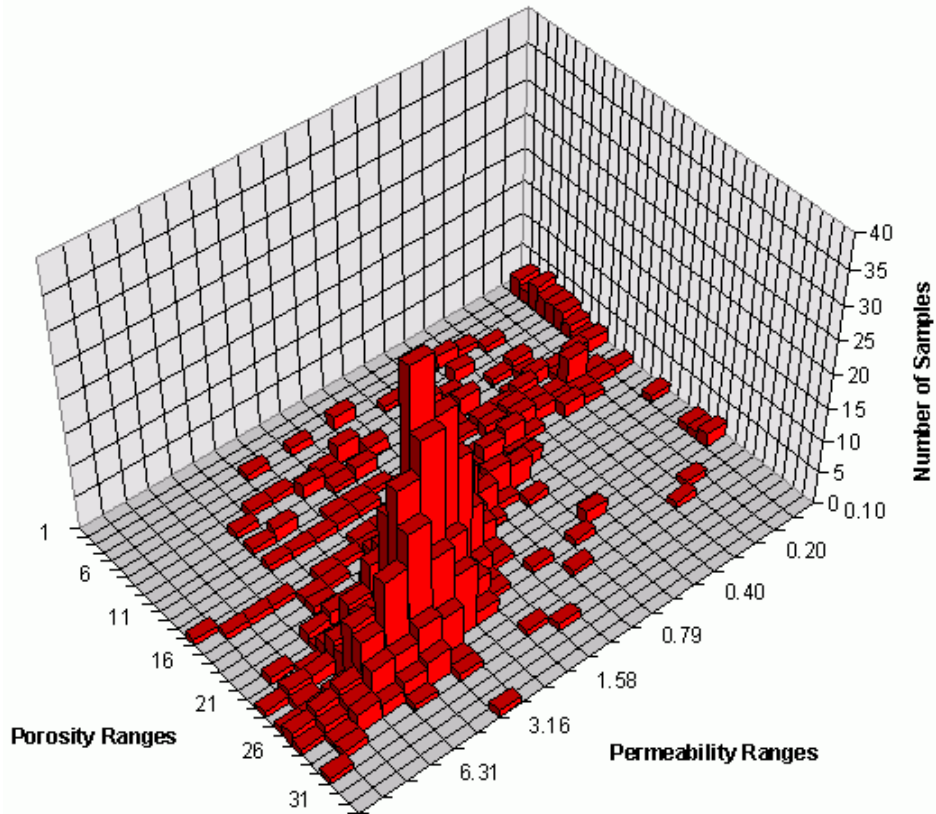


Figure 15: As above, K/Ø scales in reverse order.

are usually fully cemented (calcitic cementation related to Echinoid overgrowths). Locally some intergranular porosity may be preserved in the basal fine-grained grainstones but, due to pore-throat cementation, this lithotype behaves as a separate-vug system;

- **RO-crypto**, the mud- and wacke- stones with a cryptocrystalline matrix. It is found mainly in layer 8; there it forms a dense interval, *pro parte* the former "E- tight", between the so-called "D" and "E" reservoirs;
- **RO-crypto + Separate Vugs**, mud- and wacke- stones with a cryptocrystalline matrix and some very low to fair moldic porosity, *i.e.* a separate-vug system. It occurs in the predominantly dense limestone-dominated formation "F" below the studied interval. The common originally aragonitic bioclasts often provided some moldic porosity; unfortunately, the cryptocrystalline matrix is not permeable.

The second group corresponds to **R-chalk**, *i.e.* a nannofossil ooze matrix with fair to high porosity, but very low permeability. It is restricted to the zone "B", *i.e.* layer 1.

The third group includes 2 lithotypes, the best in terms of reservoir characteristics:

- **RR**, the mud-dominated fabric (mud-, wacke-, & pack- stones) with microcrystalline matrix and fair to high porosity values. The porosity is mainly caused by the existence of a microcrystalline matrix. It is the dominant rock-type in the porous sections of zones "C" to "E", *i.e.* in layers 2, 5, 7, 9, and 10;
- **R-stylo**, the mud-dominated fabric (mud-, wacke-, & pack- stones) with microcrystalline matrix and low to fair porosity values. This lithotype differs from the previous one because of heterogeneities within the rock, *i.e.* bedding-related stylolites that produce more tortuosity in the porous network (and also possibly because of a lesser vertical permeability range). It is found mainly in layer 6; there it forms a baffle within the so-called "D" zone, between two reservoir sub-units (layers 5 and 7).

The classification by layers into permeable or impermeable operational units has been set up to take into account both sequence stratigraphy (the "envelopes") and the dominant rock-type (the "contents"). In order to simplify its application (*i.e.* "up-scaling"), we chose a single "dominant" rock-type to characterize each layer. K/Ø cross-plots per layer (Fig. 4) and petrographic analyses support this preliminary rock-type classification. We note that RR measures differ slightly between zone "C"

(above) and zones "D-E" (below); this is possibly related to discrete depositional environments and diagenetic overprints.

Towards a refined rock-typing (from Hg injection data)

The permeability of a rock is controlled primarily by the pore-throat network, *i.e.* size, number, shape, and arrangement of pore-throats:

- The larger the passages between pores, the higher the permeability values. Permeability is strongly weighted by the larger pore-throats;
- For a given set of pore-throats, the more numerous the passages between pores, the higher the permeability values;
- Within a single rock-fabric / lithotype, it is assumed that pore-throat shape is homogenous and that pore-throats are distributed randomly.

Pore-throat sizes can be estimated from the Hg injection curves³ though these curves give only an apparent distribution (WARDLAW & TAYLOR, 1976).

Various cross-plots using factors⁴ derived from the Hg injection curves (BRC, r_{35} , etc.) illustrate that pore-throat size is the main factor controlling permeability (Fig. 2). The apparent scatter of the data is partly due to the fact that the several laboratories used divergent increments in Hg injection pressure measurements. These factors may also be involved in the way the samples are sorted (Table 1).

Here, 65 Hg injection curves were available (but 4 permeability measurements were missing because the corresponding plugs were broken: Table 1); after screening, only 7

³ E.W. WASHBURN (1921) first suggested the use of mercury injection as a laboratory method for determining pore throat size distribution. Assuming flow channels in the porous core sample may be represented by a bundle of straight capillary tubes in parallel with the spaces between the tubes sealed by a cementing material, the WASHBURN equation can be expressed as

$$P_c = -2 \gamma \left(\frac{\cos \Theta}{r} \right)$$

where P_c = capillary pressure (dynes/cm²), γ = surface tension of Hg = 480 dynes/cm, Θ = contact angle of Hg in air = 140°; and r = radius of aperture for a cylindrical pore throat. Thus,

$$r \text{ (mm)} = \left(\frac{107.744}{P_c \text{ (psia)}} \right)$$

⁴ r_{35} represents the apparent radius at 35% Hg injection (PITTMANN, 1992) while BRC is an weighted average radius also derived from the Hg injection curve.

measurements were discarded (using as a rule of thumb a $BRC \gg r_{35}$: Table 1, Fig. 3). When considering the histograms "apparent pore-throat size" versus "apparent percentage of pore volume" per layer (Fig. 8-13), *i.e.* in their relationship to the "dominant" rock-type, the following points are significant:

- The first rock-type (group of lithotypes) was all but unsampled as it characterizes the tight zones;
- The second rock-type is poorly represented, but 6 of 7 zone "B" samples (R-chalk dominant) have a $BRC < 0.15 \mu\text{m}$ ($r_{35} < 0.23 \mu\text{m}$);
- Most remaining samples (51) correspond to the third group, possibly only to lithotype RR;
- In this case, BRC values cover quite a large range, from 0.15 up to $0.77 \mu\text{m}$ ($0.23 \mu\text{m} < r_{35} < 0.93 \mu\text{m}$), but it is possible to discriminate 2 sub-groups within RR, one with $BRC < 0.3 \mu\text{m}$ (RR-"C") and another with $BRC > 0.3 \mu\text{m}$ (RR-"D-E").

Further investigations of rock-types (using statistical analyses)

As mentioned above, there are variations within lithotype RR that may justify splitting it in accordance with the origin of the sample: zone "C" or zones "D-E". However, thin sections in carbonate rocks are usually not less than $30 \mu\text{m}$ thick; the largest pore entry radius based on the Hg injection data used in the current study never exceeds $2 \mu\text{m}$ (and rarely $1 \mu\text{m}$). Consequently pore throats were not visible in thin sections. Therefore permeability and porosity distributions were examined in each layer (*i.e.* by "dominant" rock-type).

2D histograms (Fig. 8-13) show that:

- $\log K$ and \emptyset distributions follow "Gaussian" laws within each layer of the reservoir,
- average K for RR-"C" = $10^{0.25}$ (= 1.78) mD (Fig. 8-9),
- average K for RR-"D-E" = $10^{0.45}$ (= 2.82) mD (Fig. 10-13).

Frequency maps and 3D histograms (Fig. 14-15) show that:

- $\log K$ distributions are independent of \emptyset distributions (grouped shotgun plot),
- trendlines observed on the K/\emptyset cross-plot per layer / lithotype / rock-type are

misleading as they are highly weighted at one end. Consequently the coefficient of determination r^2 departs significantly from 1:

- R-chalk ("B") $K = 6.2 \cdot 10^{-3} e^{0.2232\emptyset} r^2 = 0.4268$ (438 samples)
 - RR-"C" $K = 25.6 \cdot 10^{-3} e^{0.1958\emptyset} r^2 = 0.4596$ (316 samples)
 - RR-"D-E" $K = 69.3 \cdot 10^{-3} e^{0.1532\emptyset} r^2 = 0.5043$ (901 samples)
- where K (mD) and \emptyset (%).

In conclusion, RR has to be split into RR-0.45 (= RR-"D-E") and RR-0.25 (= RR-"C") which form 2 distinct rock-types. A good match was obtained with measured depth wireline log S_w using a separate "Sw versus height" equation for each rock-type:

- **R-chalk** ("B") $\log(\emptyset S_w) = -2.159 \emptyset - 1.137 \log h + 1.746$
 - **RR-0.25** ("C") $\log(\emptyset S_w) = -4.327 \emptyset - 1.175 \log h + 1.367 \log \emptyset + 3.727$
 - **RR-0.45** ("D-E") $\log(\emptyset S_w) = -0.729 \emptyset - 0.645 \log h + 0.190 \log \emptyset + 0.338$
- where h (ft), S_w and \emptyset (fractions).

R-stylo and RR-0.45 are considered a single rock-type as the reduction in pore volume is probably restricted to the immediate vicinity of the solution seams. Presumably this reduction is accompanied only by a correlative reduction of the number of passages between pores (pore-throats). Had it been accompanied by a reduction in the size of the passages between pores, the two lithotypes would have had to remain distinct and therefore to be treated as discrete rock-types.

Conclusion (towards a new approach in rock-typing)

G.E. ARCHIE's classic paper (1950) was to some extent misinterpreted. When he wrote: "The relations between rock characteristics should be thought of as trends. Actually, these may be expressed by mathematical formulae", he immediately added the following warnings: "however, the formulae can not be applied in a rigid manner (...). It must be kept in mind that appreciable deviations from the average trend may occur".

In many studies, rock-type classifications end with trendlines drawn on K/\emptyset cross-plots with K/\emptyset transforms used to predict K from either the total or the effective \emptyset . However statistics in this presentation show that the two

Sample	Rock-Type	Porosity %	Permeability mD	BRC	R35	Status
1	R-chalk	17.3	0.10	0.124	0.146	
2	R-chalk	17.4	0.33	0.127	0.160	
3	R-chalk	14.9	0.32	0.114	0.172	
4	R-chalk	19.6	1.00	0.121	0.185	
5	R-chalk	16.1	0.13	0.147	0.188	
6	R-chalk	18.8	0.20	0.148	0.225	
7	R-chalk	16.0	0.09	0.258	0.335	
8	R-chalk	1.0	0.63	0.003	0.003	Discarded
9	RR-045	11.7	0.45	0.145	0.193	
10	RR-045	7.6	0.85	0.133	0.201	
11	RR-045	13.9	0.23	0.177	0.234	
12	RR-045	13.8	0.20	0.148	0.238	
13	RR-045	23.9	2.41	0.294	0.437	
14	RR-045	22.0	2.00	0.333	0.457	
15	RR-045	22.9	1.30	0.300	0.459	
16	RR-045	7.8	0.35	0.423	0.475	
17	RR-045	21.4	1.60	0.304	0.490	
18	RR-045	20.0	1.00	0.320	0.492	
19	RR-045	24.4	2.00	0.322	0.496	
20	RR-045	14.8	1.30	0.339	0.497	
21	RR-045	21.4	1.09	0.438	0.512	
22	RR-045	25.6	2.52	0.330	0.538	
23	RR-045	16.1	0.59	0.317	0.550	
24	RR-045	24.9	2.95	0.336	0.567	
25	RR-045	19.5	2.80	0.404	0.568	
26	RR-045	25.4	7.42	0.343	0.570	
27	RR-045	22.2	2.50	0.428	0.584	
28	RR-045	23.6	2.30	0.428	0.591	
29	RR-045	25.2	2.34	0.352	0.595	
30	RR-045	23.5	2.50	0.303	0.600	
31	RR-045	24.2	0.88	0.494	0.626	
32	RR-045	20.1	1.30	0.340	0.629	
33	RR-045	22.8	1.80	0.463	0.646	
34	RR-045	27.3	4.86	0.367	0.647	
35	RR-045	22.7	19.70	0.549	0.732	
36	RR-045	24.1	1.90	0.379	0.741	
37	RR-045	25.7	1.40	0.412	0.763	
38	RR-045	22.5	4.42	0.629	0.781	
39	RR-045	18.8	2.20	0.669	0.895	
40	RR-045	25.2	3.27	0.761	0.928	
41	RR-045	4.0	0.42	0.140	0.109	Discarded
42	RR-045	15.7	Not available	0.236	0.339	BROKEN
43	RR-045	23.5	Not available	0.273	0.407	BROKEN
44	RR-045	21.0	16.00	1.774	1.434	Discarded
45	RR-045	23.6	2.27	1.493	0.758	Discarded
46	RR-045	23.7	7.11	1.883	0.904	Discarded
47	RR-025	14.2	2.00	0.157	0.195	
48	RR-025	18.1	0.83	0.185	0.282	
49	RR-025	14.4	0.51	0.211	0.305	
50	RR-025	11.6	0.29	0.219	0.319	
51	RR-025	17.7	0.59	0.227	0.325	
52	RR-025	15.8	0.41	0.227	0.356	
53	RR-025	21.2	1.80	0.274	0.372	
54	RR-025	18.8	1.30	0.277	0.374	
55	RR-025	17.5	3.79	0.330	0.435	
56	RR-025	19.7	1.60	0.310	0.440	
57	RR-025	18.4	1.30	0.270	0.461	
58	RR-025	26.3	2.50	0.336	0.519	
59	RR-025	8.3	0.62	0.234	0.196	Discarded
60	R0-grain	9.6	0.11	0.236	0.389	
61	R0-grain	10.3	0.08	0.264	0.431	
62	R0-crypto-S.V.	20.0	2.19	0.266	0.404	Outside scope
63	R0-crypto-S.V.	18.6	4.93	0.602	0.644	Outside scope
64	R0-crypto-S.V.	12.0	Not available	0.161	0.209	Outside scope BROKEN
65	R0-crypto-S.V.	6.9	Not available	0.095	0.042	Discarded BROKEN

Table 1: List of the available P_c curves.

ranges of data do not move together; the best fits have low coefficients of determination ($r^2 < 0.5$). This problem was attacked with a different and promising approach: each rock-type appears to be characterized by Gaussian distributions of both $\log K$ and interparticle \emptyset , which as determined here almost equals the total \emptyset , and the two parameters are not correlated (Fig. 14 -15). These distributions can serve as a basis for rock-typing. Such an approach has been used earlier to describe flow in heterogeneous media (WARREN & PRICE, 1961). It is recommended that investigations be continued regarding its feasibility when applied to slightly more homogenous media, such as a single rock-type, and how the use of a geometric mean permeability value for a given rock-type effectively affects reservoir models and simulations.

Acknowledgements

The author thanks the Management of Abu Dhabi Marine Areas - Operation Company (ADMA-OPCO) and Abu Dhabi National Oil Company (ADNOC) for their permission (Ref. No.: E/OFFSH/SPG/530/99) granted to publish this paper on the occasion of the 9th ADIPEC (2000). Due to a large number of speakers attending the conferences the organizing committee decided to retain only one of the two papers offered by the author (the selected paper concerns the stratigraphy of the Thamama: GRANIER, 2000). Subsequently the remaining paper was submitted to a foreign geoscience paper-printed journal and was accepted for publication. Two years later the journal was still not issued. Therefore it is to appear in an electronic form in "Carnets de Géologie - Notebooks on Geology". Reviews of the preliminary versions by John BELLAMY and Trevor BURCHETTE resulted in many improvements to the paper. Special mention goes to Nestor J. SANDER.

References

- ARCHIE G.E. (1950).- Introduction to petrophysics of reservoir rocks. *Bulletin of the American Association of Petroleum Geologists*, Tulsa, vol. 34, N° 5, p. 943-961.
- GRANIER B. (2000).- Lower Cretaceous stratigraphy of Abu Dhabi and the United Arab Emirates - A reappraisal.- *9th Abu Dhabi International Petroleum Exhibition & Conference, Conference Proceedings*, ADIPEC 0918, Abu Dhabi, October 15th-18th, p. 526-535.
- LUCIA F.J. (1983).- Petrophysical parameters estimated from visual descriptions of carbonate rocks: a field classification of carbonate pore space. *Journal of Petroleum Technology*, Houston, vol. 35, N° 3, p. 626-637.
- LYON T.A., FULLER J., GRANIER B., HOZAYEN M., AL RIYAMI A., KHALAF A. & THIÉBOT B. (1998).- Integrated study of a faulted and fractured reservoir.- *8th Abu Dhabi International Petroleum Exhibition & Conference, Conference Proceedings*, SPE 49453, Abu Dhabi, October 11th -14th, p. 45-67.
- PITTMANN E.D. (1992).- Relationship of porosity and permeability to various parameters derived from mercury injection-capillary pressure curves for sandstone. *Bulletin of the American Association of Petroleum Geologists*, Tulsa, vol. 76, N° 2, p. 191-198.
- WARREN J.E. & PRICE H.S. (1961).- Flow in heterogeneous porous media. *Society of Petroleum Engineers Journal*, Houston, September 1961, p. 153-169.
- WARDLAW N.C. & TAYLOR R.P. (1976).- Mercury capillary pressure curves and the interpretation of pore structure and capillary behaviour in reservoir rocks. *Bulletin of Canadian Petroleum Geology*, Calgary, vol. 24, N° 2, p. 225-262
- WASHBURN E.W. (1921).- Note on a method of determining the distribution of pore sizes in a porous material. *Proceedings of the National Academy of Science of the United States of America*, Washington, vol. 7, p. 115-116.